

# Radiative falloff in black-hole spacetimes

William G. Laarakkers and Eric Poisson

*Department of Physics, University of Guelph, Guelph, Ontario, Canada N1G 2W1*

This two-part contribution to the Proceedings of the Eighth Canadian Conference on General Relativity and Relativistic Astrophysics is devoted to the evolution of a massless scalar field in two black-hole spacetimes which are not asymptotically flat.

In Part I (authored by Eric Poisson) we consider the evolution of a scalar field propagating in Schwarzschild-de Sitter spacetime. The spacetime possesses a cosmological horizon in addition to the usual event horizon. The presence of this new horizon affects the late-time evolution of the scalar field.

In part II (authored by William G. Laarakkers) we consider the evolution of a scalar field propagating in Schwarzschild-Einstein-de Sitter spacetime. The spacetime has two distinct regions: an inner black-hole region and an outer cosmological region. Early on in the evolution, the field behaves as if it were in pure Schwarzschild spacetime. Later, the field learns of the existence of the cosmological region and alters its behaviour.

## Part I by Eric Poisson

### Introduction

A theorem that establishes the uniqueness of the Schwarzschild black hole as the endpoint of gravitational collapse without rotation was proved by Werner Israel more than 30 years ago [1], and the mechanism by which the gravitational field eventually relaxes to the Schwarzschild form was elucidated by Richard Price more than 25 years ago [2]. Given the venerable age of this topic, it is surprising that more can be said about it today. Yet, many papers on radiative falloff have been written in the last few years [3–15]. Most of the new developments are concerned with rotating collapse, and how the gravitational field eventually relaxes to the Kerr form. The question we pursue in this two-part contribution is different. Focusing our attention on nonrotating black holes, we ask: How do the conditions far away from the black hole affect the relaxation process? In Part I we consider a black hole immersed in an inflationary universe. (This was first done by Brady *et al.* [14], and additional details can be found in Ref. [15].) In Part II, William G. Laarakkers will consider a black hole immersed in a spatially-flat, dust-filled universe.

### Radiative falloff in Schwarzschild spacetime

Price's result [2] can be summarized as follows. As a nonspherical star undergoes gravitational collapse, the gravitational field becomes highly dynamical, and the escaping radiation interacts with the spacetime curvature surrounding the star. At late times, well after the initial burst of radiation was emitted, the gravitational field relaxes to a pure spherical state. If  $\delta g$  schematically represents the deviation of the metric from the Schwarzschild

form, then  $\delta g \sim t^{-(2\ell+2)}$ , where  $\ell$  is the multipole order of the perturbation; the dominant contribution to  $\delta g$  comes from the quadrupole ( $\ell = 2$ ) mode.

The inverse power-law decay applies to many other situations involving radiation interacting with the curvature created by a massive object. The simplest model problem which exhibits this behaviour involves a massless scalar field in Schwarzschild spacetime. In this context, the background geometry is not affected by the field  $\Phi$ , which satisfies the wave equation

$$(g^{\alpha\beta}\nabla_\alpha\nabla_\beta - \xi R)\Phi = 0, \quad (1)$$

where  $g_{\alpha\beta}$  is the spacetime metric,  $R$  the Ricci scalar (which vanishes for Schwarzschild spacetime), and  $\xi$  a coupling constant. Because the spacetime is spherically symmetric, the field can be decomposed according to

$$\Phi = \sum_{\ell m} \frac{1}{r} \psi_\ell(t, r) Y_{\ell m}(\theta, \phi). \quad (2)$$

This leads to a decoupled equation for each wave function  $\psi_\ell$ , and we can focus on a single mode at a time.

The problem is formulated as follows. A pulse of scalar radiation (described by  $\psi_\ell$ ) impinges on the black hole and interacts with the spacetime curvature, which creates a potential barrier fairly well localized near  $r = 3M$ . The wave pulse is partially reflected and transmitted, and at late times, a tail remains. At such times, the field falls off as  $\psi_\ell \sim t^{-(2\ell+3)}$ . This is Price's power-law decay, and this behaviour is displayed in Fig. 1.

A number of analytical and numerical studies of radiative dynamics [3–7] have revealed that the inverse power-law behaviour is not sensitive to the presence of an event horizon. In fact, power-law tails are a weak-curvature phenomenon, and it is the asymptotic structure of the spacetime at radii  $r \gg 2M$  which dictates how the field behaves at times  $t \gg 2M$ . It is this observation that motivated our work: How is the field's evolution affected if the conditions at infinity are altered?

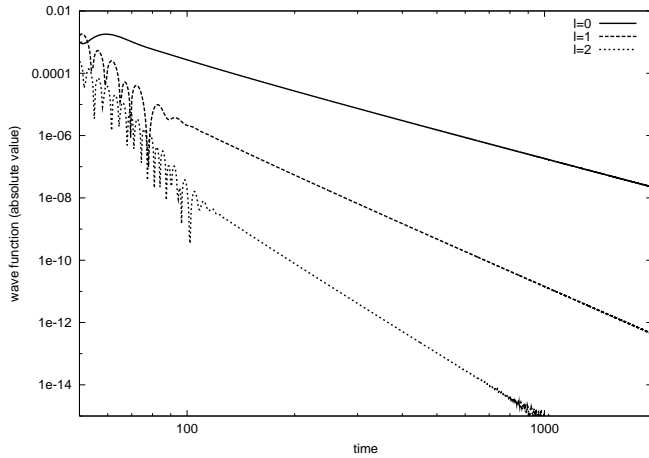


FIG. 1. Absolute value of the wave function  $\psi_\ell(t, r)$  as a function of time  $t$ , evaluated at  $r = 10$  in Schwarzschild space-time. We use units such that  $2M = 1$ . The cases  $\ell = 0, 1, 2$  are considered, and the wave functions are plotted on a log-log scale. In such a plot, a straight line indicates power-law behaviour, and a change of sign in the wave function is represented by a deep trough. We see that the field's early behaviour is oscillatory, but that it eventually decays according to an inverse power law.

### Radiative falloff in Schwarzschild-de Sitter spacetime

To provide an answer to this question, we remove the black hole from its underlying flat spacetime and place it in de Sitter spacetime, which describes an exponentially expanding universe. The Schwarzschild-de Sitter (SdS) spacetime has a metric given by

$$ds^2 = -f dt^2 + f^{-1} dr^2 + r^2 d\Omega^2, \quad (3)$$

$$f = 1 - 2M/r - r^2/a^2.$$

Here,  $a^2 = 3/\Lambda$ , where  $\Lambda$  is the cosmological constant. (The SdS metric is a solution to the modified vacuum field equations,  $G_{\alpha\beta} + \Lambda g_{\alpha\beta} = 0$ , which imply  $R = 4\Lambda = 12/a^2$ .) The spacetime possesses an event horizon at  $r = r_e \simeq 2M$  and a cosmological horizon at  $r = r_c \simeq a$ . We assume that  $r_e \ll r_c$ , so that the two length scales are cleanly separated.

We examine the time evolution of a scalar field in SdS spacetime; the field is still governed by Eq. (1), and it still admits the decomposition of Eq. (2). Figure 2 provides a comparison between the behaviour of  $\psi_\ell$  in the two spacetimes (Schwarzschild and SdS). We see that at early times, the wave functions behave identically; the field has not yet become aware of the different conditions at  $r \gg r_e$ . At later times, however, deviations become apparent. For  $\ell = 0$ , the Schwarzschild behaviour  $\psi_0 \sim t^{-3}$  is replaced by the wave function changing sign at  $t \sim 260$ , and settling down to a constant value at late times. For  $\ell = 1$ , the Schwarzschild behaviour  $\psi_1 \sim t^{-5}$

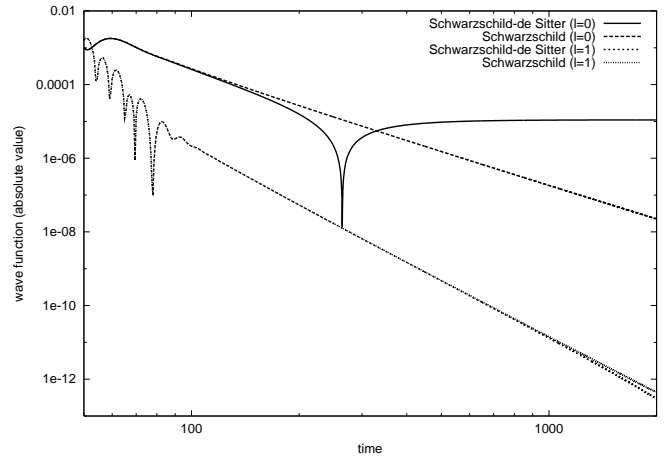


FIG. 2. Absolute value of the wave function  $\psi_\ell(t, r)$  as a function of time  $t$ , evaluated at  $r = 10$  in Schwarzschild space-time ( $r_e = 1$ ) and SdS spacetime ( $r_e = 1$  and  $r_c = 2000$ ). The cases  $\ell = 0, 1$  are considered, and the wave functions are plotted on a log-log scale. In both cases,  $\xi = 0$ .

is replaced by a faster decay which eventually becomes exponential.

The field's exponential decay is confirmed by monitoring its evolution up to times  $t > r_c$ . If  $\xi = 0$ , we find that  $\psi_\ell \sim e^{-\ell\kappa_c t}$  at late times [14], where  $\kappa_c \simeq 1/r_c$  is the surface gravity of the cosmological horizon.

A rich spectrum of late-time behaviours is revealed when  $\xi$ , the curvature-coupling constant, is allowed to be nonzero. Figure 3 shows the time-dependence of  $\psi_0$  for several values of  $\xi$ . For  $\xi$  smaller than a critical value  $\xi_c$ , the field decays monotonically with a decay constant that increases with increasing  $\xi$ . When  $\xi > \xi_c$ , however, the wave function oscillates with a decaying amplitude. As  $\xi$  is increased away from the critical value  $\xi_c$ , the frequency of the oscillations increases, but the decay constant stays the same.

This qualitative change of behaviour as  $\xi$  goes through  $\xi_c$  is quite remarkable. It can be explained with a detailed analytical calculation that will not be presented here (see Ref. [15]). This calculation reveals that at late times, the field behaves as  $\psi_\ell \sim e^{-p\kappa_c t}$ , where

$$p = \ell + \frac{3}{2} - \frac{1}{2}\sqrt{9 - 16\xi} + O\left(\frac{r_e}{r_c}\right). \quad (4)$$

This relation implies that  $p$  becomes complex, and  $\psi_\ell$  oscillatory, when  $\xi > \xi_c \equiv 3/16$ .

## Part II by William G. Laarakkers

### The spacetime

The background spacetime in which the scalar field's evolution is followed is the Schwarzschild-Einstein-de Sit-

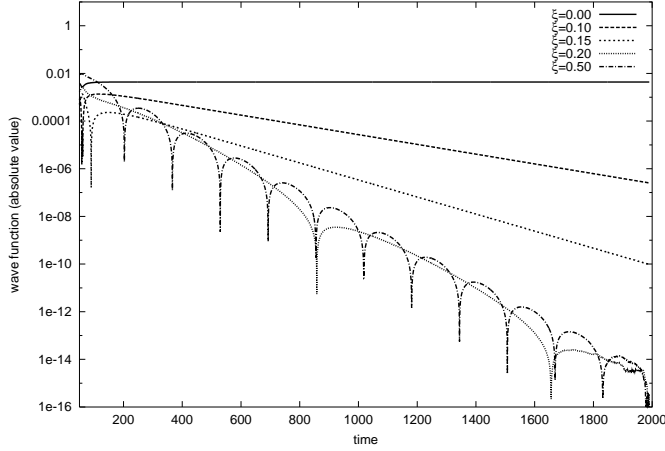


FIG. 3. Absolute value of the wave function  $\psi_0(t, r)$  as a function of time  $t$ , evaluated at  $r = 10$  in SdS spacetime ( $r_e = 1$  and  $r_c = 100$ ). Several values of  $\xi$  are considered, in the interval between  $\xi = 0$  and  $\xi = \frac{1}{2}$ . The wave functions are plotted on a semi-log scale, in which a straight line indicates exponential behaviour.

ter spacetime. Qualitatively, it can be described as follows. The idea is to start out with a spatially-flat, expanding, dust-filled universe. Then a ball of dust is “scooped” out, which leaves behind a spherical vacuum region. The dust that was removed is replaced by a Schwarzschild black hole, which is placed in the middle of the vacuous region. This produces a spacetime with two distinct regions. The inner (black hole) region is described by the Schwarzschild metric, and the outer (cosmological) region is described by the Friedman-Robertson-Walker (FRW) metric (see Fig. 4).

There are two important things to note about this spacetime. First, if the mass of the black hole is the same as the mass of the dust that was scooped out, the metric will be smooth across the boundary separating the two regions of the spacetime. Also, since the dust is pressureless it will not flow across the boundary, and the boundary itself will be co-moving with the universe.

Because the specific finite-difference equation used in the numerical work requires the use of null coordinates (see [3]), the metrics of the two regions must be put in double-null coordinate form. For the black hole region the metric is written as

$$ds^2 = -\left(1 - \frac{2M}{r}\right) du dv + r^2 d\Omega^2. \quad (5)$$

Here,  $u$  and  $v$  are ingoing and outgoing null coordinates, and  $r$  is defined implicitly by  $r + 2M \ln(r/2M - 1) = (v - u)/2$ . In the cosmological region the metric takes the form

$$ds^2 = a^2(u^*, v^*) (-du^* dv^* + \chi^2 d\Omega^2), \quad (6)$$

where  $u^*$  and  $v^*$  are ingoing and outgoing null coordinates of the FRW spacetime, different from  $u$  and  $v$ . The

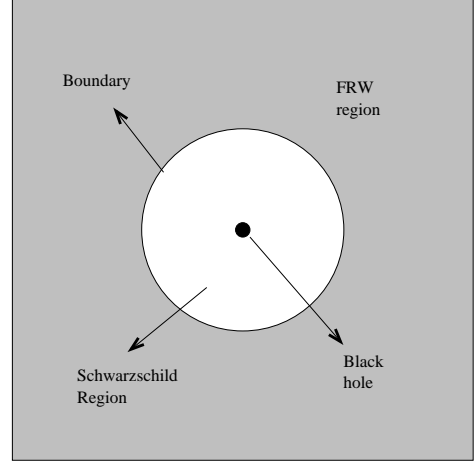


FIG. 4. Schematic of the Schwarzschild-Einstein-de Sitter spacetime. Note that the boundary between the two regions is expanding outwards, co-moving with the universe.

FRW radial coordinate is  $\chi = \frac{1}{2}(v^* - u^*)$ . The scale factor  $a$  is given by  $a(u^*, v^*) = \frac{1}{16}C(u^* + v^*)^2$ , where  $C$  is a constant that depends on the mass  $M$  of the black hole and the density of the dust.

The first task is to find one coordinate system that can describe both regions of the spacetime. This is required so that a single wave equation valid over the entire spacetime can be constructed. Since it is known that the metric is continuous across the boundary we can evaluate the metric induced on both sides of the boundary hypersurface, and set them equal. This construction allows us to find the ingoing Schwarzschild coordinate  $u$  as a function of the ingoing cosmological coordinate  $u^*$ , and the outgoing coordinate  $v$  as a function of  $v^*$ . Thus we now have a single coordinate system covering both regions of the spacetime.

### The wave equation

The wave equation that governs the evolution of the scalar field is one without curvature coupling (equivalent to setting  $\xi = 0$  (see Part I and [15])). Thus the massless scalar field  $\Phi$  obeys the equation

$$\square\Phi = g^{\alpha\beta}\nabla_\alpha\nabla_\beta\Phi = 0. \quad (7)$$

The spherical symmetry of the problem allows us to decompose the field in terms of spherical harmonics, and then to evolve only the part of the field that depends on the null coordinates. Thus the field can be decomposed as

$$\Phi = \sum_{\ell m} \frac{1}{R} \psi_\ell Y_{\ell m}(\theta, \phi), \quad (8)$$

where  $R = r$ ,  $\psi_\ell = \psi_\ell(u, v)$  in the black hole region, and  $R = a\chi$ ,  $\psi_\ell = \psi_\ell(u^*, v^*)$  in the cosmological region.

When all quantities are expressed in the starred coordinate system, each wavefunction  $\psi_\ell$  satisfies the equation

$$4 \frac{\partial^2 \psi}{\partial u^* \partial v^*} + V \psi = 0, \quad (9)$$

where the potential  $V$  takes a different form depending on which region of the spacetime the field lies:

$$V_{\text{Schild}} = \frac{du^*}{dv^*} \frac{dv}{dv^*} f \left[ \frac{\ell(\ell+1)}{r^2} + \frac{2M}{r} \right] \quad (10a)$$

$$V_{\text{FRW}} = \frac{4\ell(\ell+1)}{(v^* - u^*)^2} - \frac{8}{(v^* + u^*)^2}. \quad (10b)$$

## Results

The numerical code evaluates the field on the event horizon, on the boundary between the two regions of the spacetime, and at future null infinity. Our discussion here will be restricted to the value of the field on the event horizon for the  $\ell = 0$  and  $\ell = 1$  modes. The evolution was started at a “late” time, meaning that the boundary has expanded far enough that it can be clearly seen that the field initially behaves as it would in pure Schwarzschild spacetime. For both modes considered we see in figures 5 and 6 that the field first exhibits quasi-normal ringing followed by the well known power law decay (see, among others, [2]). However, at a certain time in the evolution, the field’s behaviour deviates from the behaviour exhibited in the pure Schwarzschild case. The point at which the field changes behaviour corresponds to the time at which information about the existence of the cosmological region reaches the event horizon.

As the wave packet falls towards the event horizon (approximated by  $u^* = u_{\text{max}}$ , where  $u_{\text{max}}$  is the largest value of  $u^*$  in the numerical grid) it encounters the localized potential (dashed line — see Fig. 7). Part of the wave is transmitted through the barrier and reaches the event horizon, and part of the wave is back-scattered by the potential. The reflected wave heads out towards the cosmological region (to the right), where it encounters the boundary  $\Sigma$ . For the  $\ell = 0$  mode the potential at the boundary is discontinuous and negative, and the field now changes sign. This sign change is the large dip in Fig. 5 (note that this is a log scale, so that as the field passes through  $\psi = 0$  the logarithm goes to negative infinity). It is when this information reaches the event horizon that the evolution of the field deviates from its evolution in pure Schwarzschild spacetime. The field continues to decay with a power-law falloff, but the falloff is much slower than in the pure Schwarzschild case.

The discussion for the  $\ell = 1$  case is similar, until the reflected wave reaches the boundary  $\Sigma$ . This is because the potential at the boundary is discontinuous and *positive* for  $\ell > 0$  (see equation 10b). Therefore the field will be partially transmitted through the barrier at the

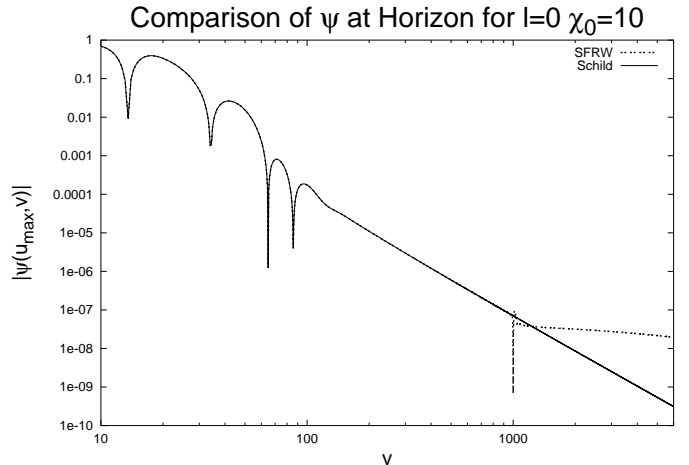


FIG. 5. Absolute value of the field on the event horizon as a function of  $v$ , for  $\ell = 0$ . The solid line is the evolution of the scalar wave in pure Schwarzschild spacetime. The dashed line is the evolution in the Schwarzschild-Einstein-de Sitter spacetime. The sharp dip near  $v = 1000$  is where the field learns about the boundary  $\Sigma$  and changes sign. Before this point, the field decays as  $\psi \sim v^{-3}$ . After this point, the field decays as  $\psi \sim v^{-1}$ .

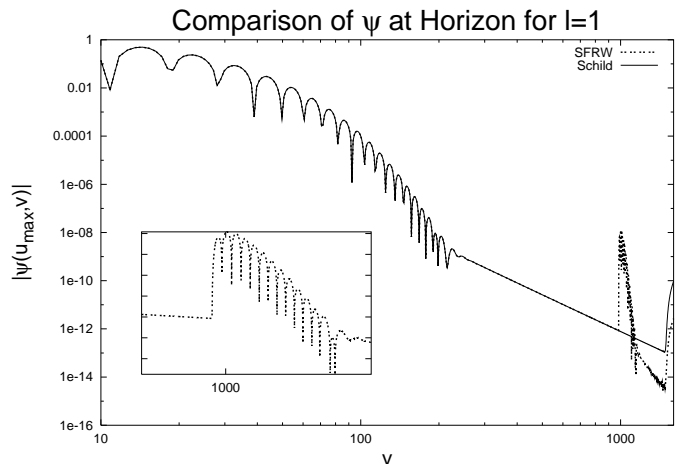


FIG. 6. Absolute value of the field on the event horizon, as a function of  $v$  for  $\ell = 1$ . The solid line is the evolution in pure Schwarzschild spacetime. The dashed line is the evolution in the Schwarzschild-Einstein-de Sitter spacetime. The inset is a close-up of the region near  $v = 1000$  where the field learns about the boundary  $\Sigma$ . Echoes of the quasi-normal oscillations in the field can be seen.

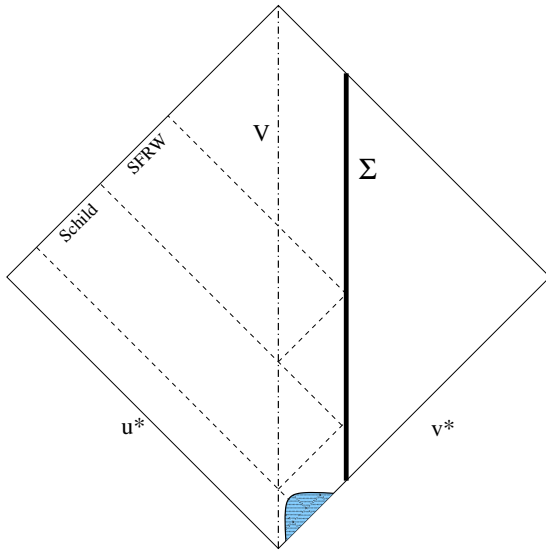


FIG. 7. Evolution of the scalar field. Here the boundary between the two spacetimes is the line  $\Sigma$ , with the black hole region to the left and the cosmological region to the right. The line marked  $V$  represents the maximum of the potential. The dashed lines are the reflection and transmission of the wave pulse from the potential and the boundary. At the event horizon the field initially behaves as if it were in pure Schwarzschild spacetime (Schild), then evolves differently (SFRW).

boundary and partially reflected off. The transmitted wave will make its way off to future null infinity. As for the part of the wave packet that has now been reflected twice, it will fall back towards the black hole where it once again encounters the localized potential. The part of the wave that manages to make it through the potential on its second encounter heads back towards the event horizon, carrying information about the existence of the boundary. This second encounter with the localized potential has the same effect on the packet as it did the first time—namely, the field again exhibits quasi-normal ringing (see inset of Fig. 6). This “echoing” phenomenon occurs only for the  $\ell > 0$  modes of the field.

## ACKNOWLEDGMENTS

The work presented in Part I was carried out in collaboration with Patrick Brady and Chris Chambers; additional details can be found in Ref. [15]. This work was supported by the Natural Sciences and Engineering Research Council.

- 
- [1] W. Israel, Phys. Rev. **164**, 1776 (1967).
  - [2] R.H. Price, Phys. Rev. D **5**, 2419 (1972); **5**, 2439 (1972).
  - [3] C. Gundlach, R.H. Price, and J. Pullin, Phys. Rev. D **49**, 883 (1994); **49**, 890 (1994).
  - [4] L.M. Burko and A. Ori, Phys. Rev. D **56**, 7820 (1997).
  - [5] E.S.C. Ching, P.T. Leung, W.M. Suen, and K. Young, Phys. Rev. Lett. **74**, 2414 (1995); Phys. Rev. D **52**, 2118 (1995).
  - [6] N. Andersson, Phys. Rev. D **55**, 468 (1997).
  - [7] L. Barack, Phys. Rev. D **59**, 044016 (1999); 044017 (1999).
  - [8] L. Barack and A. Ori, gr-qc/9902082; gr-qc/9907085.
  - [9] S. Hod and T. Piran, Phys. Rev. D **58**, 024017 (1998); **58** 024018 (1998); **58** 024019 (1998); **58**, 044018 (1998).
  - [10] S. Hod, Phys. Rev. D **58**, 104022 (1998); gr-qc/9902072; gr-qc/9902073; gr-qc/9907044; gr-qc/9907096.
  - [11] W. Krivan, P. Laguna, and P. Papadopoulos, Phys. Rev. D **54**, 4728 (1996).
  - [12] W. Krivan, P. Laguna, P. Papadopoulos, and N. Andersson, Phys. Rev. D **56**, 3395 (1997).
  - [13] W. Krivan, gr-qc/9907038.
  - [14] P.R. Brady, C.M. Chambers, W. Krivan, and P. Laguna, Phys. Rev. D **55**, 7538 (1997).
  - [15] P.R. Brady, C.M. Chambers, W.G. Laarakkers, and E. Poisson, gr-qc/9902010.